PROTEINS: Structure, Function, and Genetics 39:26–36 (2000)

Conformational Flexibility of the Catalytic Asp Dyad in HIV-1 Protease: an Ab Initio Study on the Free Enzyme

Stefano Piana,[1] and Paolo Carloni[1,2]*
[1]*International School for Advanced Studies and Istituto Nazionale di Fisica della Materia, Trieste, Italy*
[2]*International Centre for Genetic Engineering and Biotechnology, AREA Science Park, Trieste, Italy*

ABSTRACT **The enzyme protease from the human immunodeficiency virus type 1 (HIV-1 PR) is one of the main targets for therapeutic intervention in AIDS. Computer modeling is useful for probing the binding of novel ligands, yet empirical force field-based methods have encountered problems in adequately describing interactions of the catalytic aspartyl pair. In this work we use ab initio dynamic methods to study the molecular interactions and the conformational flexibility of the Asp dyad in the free enzyme. Calculations are performed on model complexes that include, besides the Asp dyad, the conserved Thr26 and Gly27 residues and water molecules present in the active site channel. Our calculations provide proton location and binding mode of the active-site water molecule, which turn out to be different from those of the eukariotic isoenzyme. Furthermore, the calculations reproduce well the structural features of the aspartyl dyad in the protein. Finally, they allow the identification of both dipole/charge interactions and a low-barrier hydrogen bond as important stabilizing factors for the peculiar conformation of the active site. These findings are consistent with site-directed mutagenesis experiments on the 27, 27′ positions (Bagossi et al., Protein Eng 1996;9:997–1003). The electric field of the protein frame (included in some of the calculations) does not affect significantly the chemical bonding at the cleavage site. Proteins 2000;39:26–36.** © 2000 Wiley-Liss, Inc.

Key words: density functional theory; molecular dynamics; protease; human immunodeficiency virus type 1; protonation state; low-barrier hydrogen bond

INTRODUCTION

The enzyme protease from the human immunodeficiency virus type 1 (HIV-1 PR) homodimeric enzyme cleaves to the multidomain protein encoded by the virus genome to yield separated structural proteins and enzymes.[2]

Since the discovery that inactivation of the enzyme results in the production of noninfectious HIV particles,[3–5] tremendous progress has been made in designing anti-AIDS drugs thanks to the determination of the three-dimensional structures of the enzyme alone and complexed with a large number of inhibitors.[6–16]

From these studies, it soon became evident that in the substrate-cleavage site—two Asp-Thr-Gly loops at the subunit-subunit interface (Chart I)—the almost coplanar conformation of the catalytic Asp dyad is crucial for the enzymatic function and for the binding of both substrate and inhibitors.[17–19]

Based on these structures, classical molecular mechanics/dynamics calculations have been performed to provide a description of enzyme-substrate interactions and to predict ligand affinities.[20–28] However, these approaches have encountered difficulties in modeling the active site: from reproducing the correct positioning of the Asp dyad to providing location and parameterization of the proton(s) shared by the Asp pair in unbound and in complexed protein.[29,30] As a result, ad hoc assumptions have often been introduced in the calculations: from choosing approximate charge distributions[24] to imposing geometric constraints between the carboxylate moieties[25,26] and to positioning the proton midway between the two adjacent Asp groups.[28] These a posteriori models, therefore, do not provide the chemical-physical origin of the stability in the active site.

Accurate quantum mechanical methods provide an alternative frame to investigate the conformational flexibility of the Asp dyad in HIV1-PR. Up to now, quantum mechanical calculations have been performed on relatively large models at the semiempirical level[13,26] and on smaller fragments at the ab initio level.[31–37] These studies provided useful information on the reaction pathways, yet quantitative conformational analysis was prevented by their accuracy[36] or the limited size of the system.

In this work, we use ab initio molecular dynamics (MD) simulations[38] to provide an understanding of the molecular interactions of the Asp dyad in the free (i.e., unbound) enzyme. This technique appears to be favorable in several respects. On the basis of state-of-the-art density functional theory calculations, it ensures a reliable description of the interactions and the charge distribution for rather large systems. Furthermore, temperature effects, of utmost importance for biological function,[39] are fully included.

Grant sponsor: COFIN—Ministero dell Università e della Ricerca Scientifica.

*Correspondence to: Paolo Carloni, International School for Advanced Studies (SISSA/ISAS), via Beirut 4, I-34014 Trieste, Italy. E-mail: carloni@sissa.it

Received 29 June 1999; Accepted 12 October 1999

Finally, its present implementation with a planewave basis set and BLYP gradient correction[40,41] for the exchange-correlation functional has been shown to treat H-bonded systems with good accuracy[42–44] and has already been applied successfully to other enzymatic systems.[45]

Our investigation is divided in two steps. First, we attempt to determine the proton location in the cleavage site.[29,30,46] Then, we perform ab initio MD to study the conformational flexibility of the Asp dyad of HIV-1 protease on models of increasing complexity and also with the inclusion of the protein electrostatic potential.

We find that the proton location and the H-bond pattern at the cleavage site of free HIV-1 PR differs from what has been found for the free eukariotic isoenzyme; furthermore, we identify a low-barrier hydrogen bond and charge dipole interactions as important factors for the Asp dyad stability. Finally, we find that polarization effects of the entire protein on the cleavage site do not affect significantly the intermolecular interactions between the two closely opposed Asp groups.

METHODS

Structural Models

Complexes **A** and **B–C** were considered for the deprotonated and monoprotonated forms, respectively (Fig. 1). Note that protomers, in which the proton is located on Oδ2(Asp 25) or Oδ1(Asp 25), are equivalent to **B** and **C,** respectively, because of the chemical equivalence of the two Aspartyl groups in the free enzyme.

Complexes **A, B,** and **C** included Asp 25(25′), modeled as an acetic acid/acetate molecules; the Thr 26(26′)-Gly 27(27′) peptide bonds, modeled as N-methyl acetamide; and three water molecules present in the active site channel (Chart I).

The complexes were constructed starting from the structure of the free enzyme (3PHV entry in the PDB database, 2.7 Å resolution[9]). High-resolution structures of HIV-1 PR-inhibitor adducts (2.3–1.8 Å of resolution)[13–16] exhibit similar conformation, the rms deviations in the catalytic triad (i.e., Asp25(25′), Thr26(26′), and Gly27(27′)) ranging from 0.4 to 0.5 Å.

From the X-ray structure, it is known that a water molecule bridges the two Asp groups (Wat_b hereafter), even though its exact location has not been provided. We positioned Wat_b to form H-bond patterns already proposed for the eukariotic isoenzyme.[37]

Other water molecules, present in the active site channel of the free enzyme and not detected by the X-ray diffraction experiment, may bind to the Asp dyad. To determine number and position of these waters, we performed classical molecular dynamics simulations using the AMBER 5.0 suite of programs.[47] The protein was immersed in a 6.0 Å-thick shell of 1070 water molecules. The protein net charges of +4 (containing the deprotonated Asp dyad) and +5 (containing the monoprotonated Asp dyad) were neutralized by adding chlorine counterions close to Arg 41, Lys 55, Lys 70, Arg 41′, Lys 70′. The positions of the hydrogen atoms and of all the water molecules but Wat_b were kept fixed in their starting position. For the three systems, 10,000 steps of geometry optimization based on the AMBER[47] force field were carried out. Then, the systems underwent 2 ps classical molecular dynamics simulation at 150 K and 100 ps at 300 K. The systems were coupled to a thermal bath[48] with relaxation time 0.2 ps. The average number of waters interacting with the Asp dyad was calculated by using the CARNAL module of AMBER.[47] For each step of the simulation, a water-Asp H-bond was considered to be formed if $d(O\delta2_{Asp}–O_{Wat}) \leq 3.5$ Å and $\angle(O\delta2_{Asp}–H_{Wat}–O_{Wat}) \geq 60°$.

In all circumstances two water molecules, besides Wat_b, interact with the Asp dyad. Thus, three water molecules were added in complexes **A, B,** and **C** (Chart I).

Complexes **C(I)** and **C(II)** (Chart I) differ from **C** for the Thr26(26′)-Gly 27(27′) moiety: this was omitted in **C(I)** and modeled as dimethylamine in **C(II).** Complexes **C(III)** and **C(IV)** (not shown) differ from **C** for the number of water molecules: two in **C(III)** and one in **C(IV).**

Quantum Mechanical Calculations

The quantum problem was solved within the density functional theory framework. The exchange and correlation functionals were those of Becke[40] and Lee et al.,[41], respectively, which are known to give optimal results for hydrogen-bonded systems.[42–44] The interactions between valence electrons and ionic cores were described by pseudopotentials by Troulliers and Martins.[49] The Kohn-Sham orbitals were expanded in plane waves up to 70 Ry. The complexes were treated as isolated systems as in Barnett and Landman.[50] The charges of the models was set to −1 for the protonated form and −2 for the deprotonated form.

Geometry optimizations were performed on protomers **B, C,** and on the deprotonated form **A** (Fig. 1) by using the direct inversion in the iterative subspace method.[51]

Ab initio molecular dynamics simulations were performed following the Car-Parrinello scheme.[38] A time step of 0.096 fs and a fictitious electron mass of 400 a.u were used. The systems were coupled to a Nose' thermostat of 500 cm^{-1} frequency and first heated to 150 K for 0.1 ps and then kept at 300 K.

To not increase excessively the computer time, the simulations of complexes **C(I)** and **C(II)** were stopped as soon as they resulted in a highly distorted structure; the simulations of complexes **C, C(III),** and **C(IV),** which resulted in a stable structure, were prolonged until proton hopping was observed. As a result, overall trajectories of 0.9, 0.9, 0.9, 1.0, 2.5, and 4.5 ps were collected for complexes **A, C(I), C(II), C(IV), C(III),** and **C,** respectively.

The positions of the hydrogen atoms replacing the protein backbone Cα atoms were kept fixed to mimic the presence of the protein frame. These constraints left the carboxylate group quite flexible and free to rotate. Also, the position of the terminal backbone atoms of Gly 27(27′) and Thr 26(26′) were kept fixed, to mimic the effect of the rest of the backbone. The latter is very rigid in that region because of a characteristic hydrogen bond network present in both free and complexed protein.[6–12]

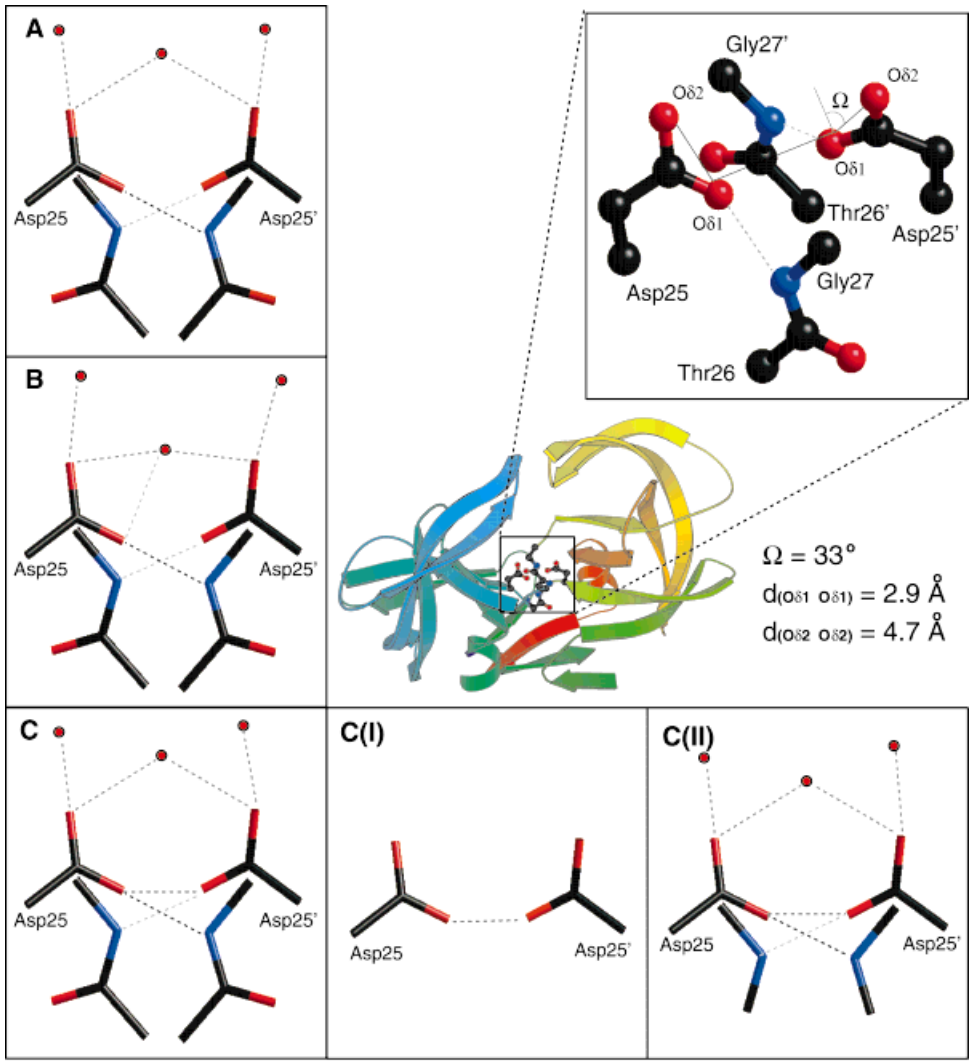

Chart I. HIV-1 Protease[9] and its active site; model complexes used in the quantum mechanical calculations are also shown. Hydrogen atoms are not shown for clarity.

All the quantum-mechanical calculations use the CPMD V3.0h[52] and required approximately 800 cpu hours on a 32-nodes Cray T3e machine.

Calculated Properties

Electrostatic interaction energies of the Thr26-Gly27 peptide unit with the aspartyl pair (in **C**) and of one Asp group with the other (in **A**) were estimated by using the atomic ESP charges[53] and assuming a dielectric constant $\epsilon = 1$.

Binding energies, i.e. the energy differences between the whole model and the elements forming it (Asp dyad and Thr26-Gly 27 peptide units) could not be calculated because of the instability of one fragment, the Asp dyad.

The electrostatic potential Φ generated by the protein/water system (obtained by geometry optimization of the MD structure [see above]) was calculated as:

$$\Phi(r) = \sum_i \frac{q_i}{r_i - r}$$

where q_i are the RESP[54,55] atomic point charges at the atomic positions r_i.

Velocity autocorrelation functions (*VAC*) were calculated as[56]:

$$VAC(t) = \frac{1}{t_{max}} \sum_{t_0=1}^{t_{max}} V(t_0)V(t_0 + t)$$

where $t_{max} = 2.25$ ps. The correspondent power spectrum was obtained as the Fourier transform of the *VAC*. The frequency interval for the transformation was set to 10 cm^{-1}. The contributions of specific atoms were calculated by projecting the *VAC* on these atoms.

The centers of the maximally localized Wannier orbitals[57,58] were calculated as previously reported.[59,60] In

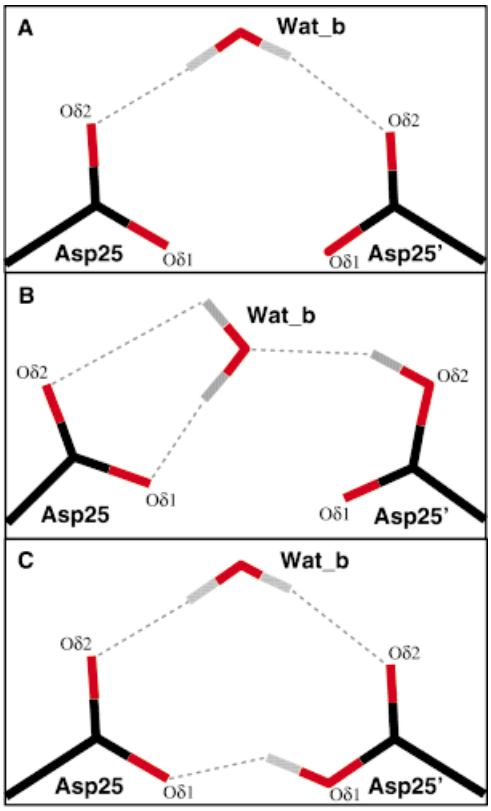

Fig. 1. Protonated and deprotonated forms of the Asp dyad. Protomers **B** and **C** are characterized by different water and proton positions, whereas **A** is the deprotonated form. Thr 26(26′)-Gly 27(27′) residues, and the two water molecules of the active site channel interacting with the Asp dyad are not shown for clarity.

particular, we relate the positions of the centers of chemical bonds to the differences of Pauling electronegativity[61] between the two atoms forming the bond.[59]

The root mean square deviation (rmsd) between two fitted structures of coordinates $\bar{r}_{i1}$ and $\bar{r}_{i2}$ was calculated as:

TABLE I. Selected Structural Parameters Resulting From Geometry Optimizations of Complex A, B, and C Compared with the Experimental Structure

Measure	Exp.	A	B	C
Oδ2-Oδ2	4.87	7.59	5.70	4.64
Oδ1-Oδ1	2.95	5.34	3.98	2.51
Cγ-Cγ	4.70	6.81	5.52	4.60
$O\delta1_{Asp25}$-N_{Gly27}	2.55	1.92	2.90	2.83
$O\delta1_{Asp25'}$-$N_{Gly27'}$	2.55	2.28	2.83	2.87
ω	33°	21°	48°	29°
rmsd	—	1.16	0.59	0.26

$$rmsd = \sqrt{\sum_i \frac{(\bar{r}_{i1} - \bar{r}_{i2})^2}{n}}.$$

RESULTS

In this section, we present our investigation on the protonation state and on the dynamics of the Asp dyad in free HIV-1 PR.

Protonation State of Free HIV-1 PR

At optimal pH for enzymatic activity (~5–6),[29,30,62] the Asp dyad can in principle exist in three protonation states, a deprotonated, a monoprotonated, and a diprotonated form. In the case of inhibitor-enzyme complexes, the protonation state depends on the type of inhibitor.[63–67] Hydrogen atoms are invisible in the X-ray structures of the enzyme alone and complexed with inhibitors[6–16]; evidence for a specific protonation state can be inferred indirectly by spectroscopic or titration measurements and by theoretical calculations.

Up to now, the existence of the diprotonated form has not been proposed for the free enzyme. In contrast, there is strong evidence from both experiment and theory that in the free enzyme the Asp dyad is monoprotonated at pH 5–6. Indeed, enzymatic kinetic experiments[29] and Poisson-Boltzman electrostatic calculations[46] have yielded a consistent picture in which the pK_as of the Asp dyad are ~3

Fig. 2. Comparison of the ab initio energy minimized structures of complexes **A, B,** and **C** (thick lines) with the X-ray structure (thin line)[9]; only the Asp dyad and Wat_b are shown for clarity. The electron density resulting from the X-ray diffraction experiments is also plotted (Abstracted with permission from Wlodawen et al.,[7] copyright 1990 American Association for the Advancement of Science).

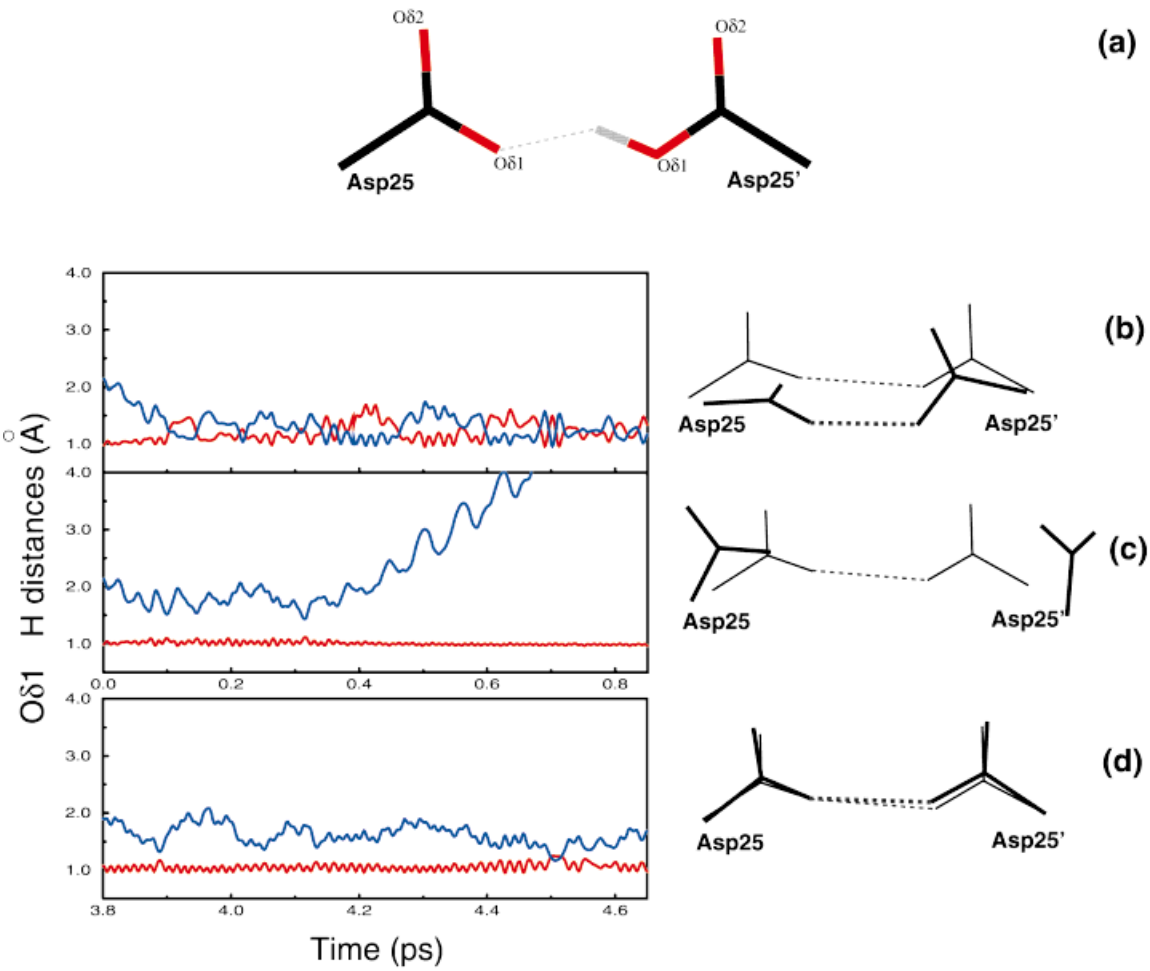

Fig. 3. Ab initio molecular dynamics of complexes **C(I), C(II),** and **C. a:** Location of the proton; **b–d:** (Left) Oδ1 · · · H distances plotted as a function of time and (right) final (thick line) and starting (thin line) structures of complexes **C(I)** (b), **C(II)** (c), and **C** (d). In (d, left) only the last 0.9 ps are shown.

and ~6. Thus, the fraction of monoprotonated species is expected to be predominant at pH 5–6.

The existence of the deprotonated form is supported only by a recent NMR study[30] at pH 6. However, this study has been subjected to criticism[46] and it is not conclusive.

To consider all the possible protonation states that have been supported or postulated for the free enzyme, we have, therefore, performed calculations on the deprotonated species **A** and the protonated forms **B-C.**

Structure and Dynamics of the Deprotonated Species

To explore the stability of the putative dinegative Asp pair,[30] we performed geometry optimization and 0.9 ps of ab initio molecular dynamics of complex **A.** After the minimization, the two negatively charged aspartyl groups rearranged to an unphysical distorted conformation (rmsd 0.5) (Table I). Figure 2 compares the electronic density and the structure of the aspartyl dyad obtained by X-ray diffraction with the optimized structure. We note that the distortion is rather large and that Wat_b is located far from the experimental electron density. During the dynamics even more dramatic rearrangements are experienced (rmsd after the simulation 1.16).

The highly distorted conformation is a consequence of the strong Asp-Asp repulsion, which turns out to be approximately +30 kcal/mol. Inspection of the X-ray structure[7,9] shows that no polar or charged residues interact with the Asp pair to counterbalance the strong Asp-Asp repulsive interaction. Thus, we expect that the result is not significantly affected by using larger models of the cleavage site.

In conclusion, our results indicate that the Asp25-Asp25′ complex is unstable in the deprotonated state.

Location of the Proton in the Monoprotonated Form

Because of the chemical equivalence of the two aspartyl groups in HIV-1 protease, only the two protomers **B** and **C** have to be considered for the monoprotonated species (Fig. 1).

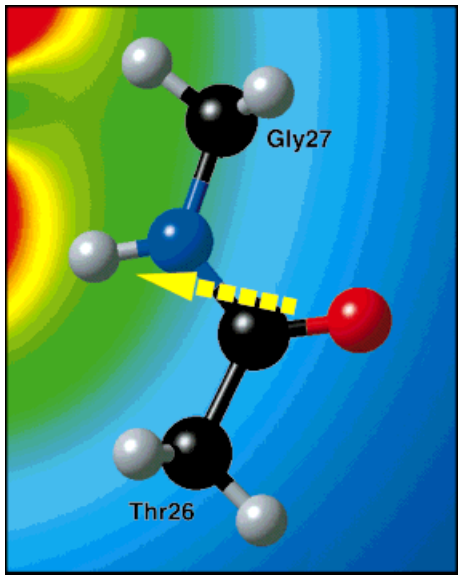

Fig. 4. Thr26-Gly 27 peptide unit's dipole (calculated and experimental[75] values 3.82 D and 3.84 D, respectively) superimposed on the electrostatic potential of the Asp dyad active site. The coloring varies continuously from red in negative areas to blue in more positive regions.

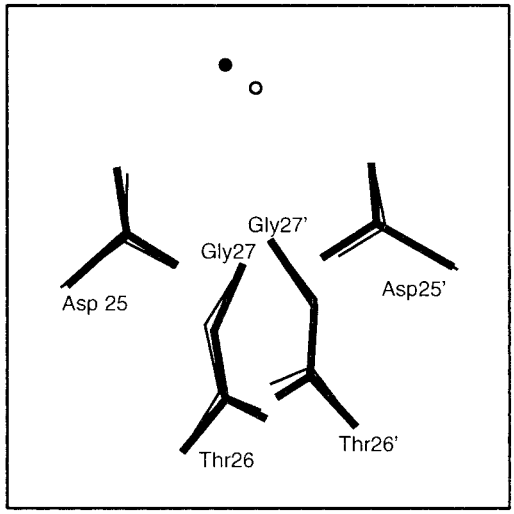

Fig. 5. Comparison between initial (thin line) and final (thick line) structures of **C.** Only Wat_b is shown for clarity.

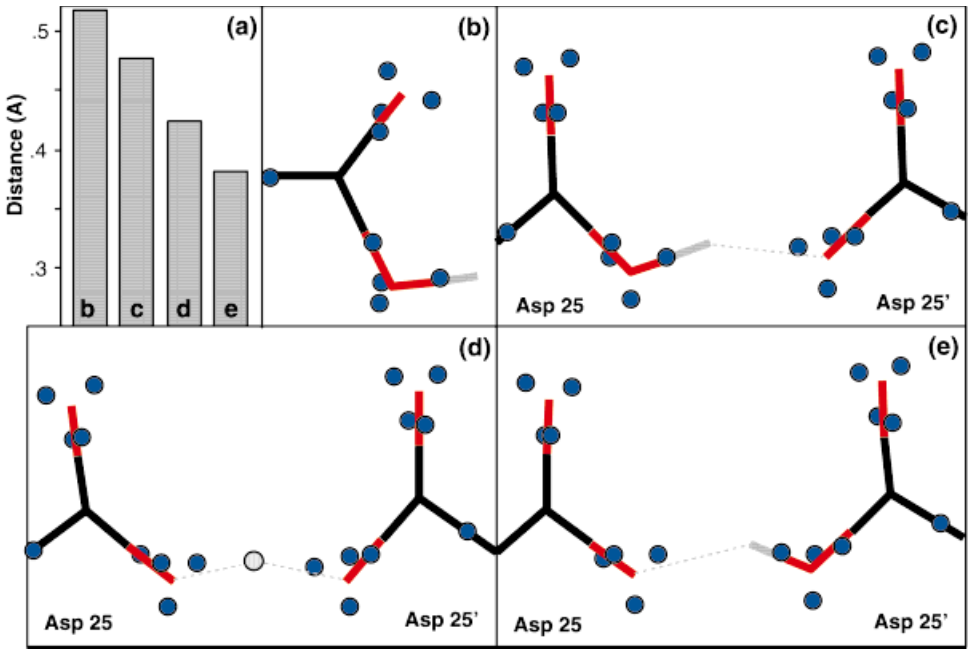

Fig. 6. Proton transfer process. **a:** Distance between Oδ2 and the center of the maximally localized Wannier function along the Oδ2-H bond in different chemical environments (**b**)–(**e**). Centers of Wannier orbitals in isolated, protonated aspartic acid (b) and in HIV-1 PR active site, before (c), during (d), and after (e) the proton transfer. The centers of the Wannier orbitals are drawn as blue circles.

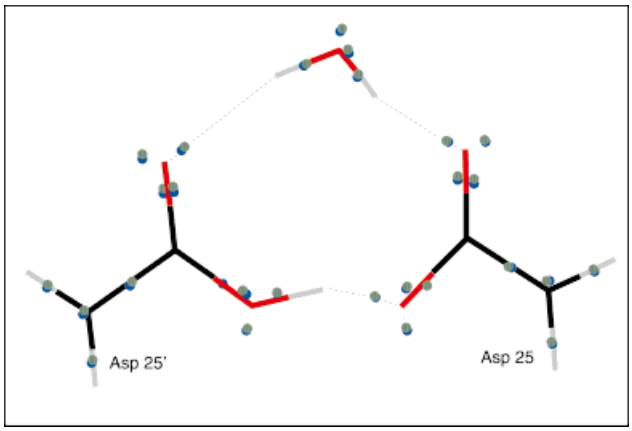

Fig. 7. Orbital polarization induced by the electrostatic field of the protein/water environment. The centers of the Wannier orbitals are indicated by blue (green) spheres for the calculations with (without) protein electrostatic potential.

In eukaryotic aspartyl proteases (E-PR), high-level ab initio calculations have established that the proton is located on the Oδ2 position[37] and that the water molecule bridging the two Asp group (Wat_b) forms three hydrogen bonds with the Asp dyad (protomer **B** in Fig. 1).

However, in HIV-PR the structural properties and the chemical environment of the aspartyl dyad are rather different from those of the eukaryotic isoenzyme. Indeed, the carboxylates are closer and less coplanar than in the eukaryotic enzymes[68] (angle between carboxylates Ω (33°) and Oδ2-Oδ2 distance (4.8 Å) compared with 8° and 5.7 Å in pepsin and 18° and 5.8 Å in endopepsin); furthermore, the electronic densities maps of HIV-1 and E-PRs are suggestive of different locations of Wat_b.[7] (Quantitative comparison cannot be made because the structural parameters of Wat_b have not been deposited.[6,7]) Finally, in HIV-1 PR there are no polar or charged groups interacting with the aspartyl dyad, in contrast to E-PRs, where conserved Ser residues H-bond to the Oδ2 oxygens.

The different chemistry at the cleavage site of the two enzymes could result in different energetics. Thus, we undertook ab initio energy calculations on both protomers of HIV-1 PR to establish which form is the most stable.

The ab initio energy minimizations performed on relatively large models of the two protomers **C** and **B** (Chart I) indicate that (a) **C** is lower in energy than **B** by 1.1 kcal/mol; (b) conformation of **C** is close to the X-ray structure but that of **B** is not (Table I and Fig. 2); and (c) the location of Wat_b is close to the electronic density in **C** but not in **B** (Fig. 2). Inclusion of additional water molecules of the active site channel is expected to stabilize further protomer **B** relative to **C** because Wat_b can form additional H-bonds to the solvent in **C** and not in **B.** (Ab initio energy minimizations of the four different possible protomers of endothiapepsin provided evidence that in this protein **B** is more stable than **C,** in agreement with previous findings.[37])

Why then is the proton located differently in HIV-1 and eukaryotic proteases? A possible explanation is offered by the different structural properties of the two classes of isoenzymes. As mentioned above, in endothiapepsin and pepsin the Oδ2-Oδ2 distances are larger than those in HIV-1 PR; thus, in protomer **C,** Wat_b can form two H-bonds with the Oδ2 atoms in HIV-1 PR, but only one in endothiapepsin and pepsin, because of longer Wat_b-Oδ2 distances.

In conclusion, our calculations suggest that the conformation of the Asp dyad in the deprotonated form is not stable. Instead, our calculations provide strong evidence in favor of the presence of protomer **C** in free HIV-1 PR.

All the subsequent calculations have been performed on complex **C** itself or its derivatives.

Ab Initio MD Simulations on the Monoprotonated Form

To study the influence of interacting groups on the conformational flexibility of the Asp dyad, we performed simulations at room temperature on model complexes at different levels of sophistication (Chart I): from the simple Asp dyad (**C(I)**) to a hydrated system that includes the glycine amide-carboxylate hydrogen bonds (thought to be important for stabilizing the Asp dyad[6,32,69]) (**C(II)**), to complex **C** which fully includes the Thr 26-Gly 27 peptide link.

The ab initio MD simulation of the simple Asp dyad—Complex **C(I)** (Chart I)—indicates a hopping of the aspartyl proton between the oxygen atoms already on the subpicosecond timescale (Fig. 3b): the two Oδ1 atoms oscillate around a very short equilibrium distance. The presence of this low-barrier hydrogen bond (LBHB) confirms previous findings based on quantum dynamical studies.[36] During the dynamics, the LBHB appears to compensate for the strong repulsion between the two Asp Oδ1 atoms (Oδ1-Oδ1 average distance 2.5(0.1) Å), which is consistent with the suggestion that this type of interaction can provide several kcal/mol of energy stabilization.[70,71]

Although the LBHB is maintained during the entire simulation, the rest of the complex is unstable on the subpicosecond timescale: after 0.2 ps the two aspartates begin to rotate around the Cβ-Cγ bond and, at the end of the simulation, the coplanarity is completely disrupted (Fig. 3b) (Ω = 70°). Conformational energy calculations indicate that the final structure is lower in energy by as much as 4.1 kcal/mol relative to the initial conformation of the protein.

We conclude that the LBHB bond is able to keep the proton-sharing oxygen atoms close to each other, but the repulsion of the other oxygens of the carboxylates renders the system unstable.

Inclusion of hydration and the hydrogen bond interaction with the glycine residues—Complex **C(II)** (Chart I)—is not sufficient to produce a stable conformation: besides the loss of the characteristic orientation of the Asp groups after ≈0.25 ps (Ω = 60°), also the Asp-Asp hydrogen bond is disrupted (Fig. 3c): the distance between the Oδ1 atoms increases from 2.1 to 7.0 Å. Fig. 3c shows that in the last configuration, the Asp groups point toward the solvent and also that the hydrogen bond between Asp 25′ and Gly 27′ is broken (Oδ1 · · · H(N) distance 4.1 Å).

Inspection of the X-ray structures of unbound and complexed HIV-1 PR[6–14] offers an explanation for the instability of the system: in every structure investigated, the rather rigid Gly amide groups do not form an optimum hydrogen bond with the Asp groups, ∠(N-H · · · Oδ1) ranging from 125 to 153°). As a result, after ≈0.4 ps, the carboxylate groups rearrange unphysically to maximize the hydrogen bonds (maximum ∠(N-H · · · Oδ1) = 179°) to destroy the aspartyl hydrogen bond. Thus, we conclude that H-bonding to Gly27(27′) is not an essential factor for the stability of the Asp dyad.

What then are the key interactions stabilizing the conformation as it is found in the experimental structures? A detailed inspection of the active site suggests the strong dipoles of the Thr 26(26′) - Gly 27(27′) peptide units as important factors, because they point toward the negative charge of the Asp dyad. Indeed, calculation of the aspartyl dyad quantum mechanically derived electrostatic potential reveals a striking alignment of the peptide unit dipoles

with the Asp charge (Fig. 4). The resulting electrostatic interaction is rather large (estimation from a point charge model −7.8 kcal/mol).

The new simulation, where the peptide link is also included—Complex C (Chart I)—confirms the fundamental role of the charge-dipole interactions. Indeed, the system is stable over the relatively long-range time explored (>4.5 ps) (Figs. 3d and 5).

Importantly, the Asp dyad keeps its coplanarity (Ω = 28(16)°). During the dynamics, the water molecules experience large mobility, forming and breaking hydrogen bonds with themselves and with the Asp dyad. In particular, the water bridging the two Asp groups (Wat_b, Fig. 1) exchanges with the other water molecules. On average, the neutral and negative Asp groups form one and two hydrogen bonds to the solvent, respectively, as shown by the radial distribution functions.

Also in this complex, proton hopping between the carboxylate groups is observed. The timescale of the process is significantly longer (Fig. 3d) as a consequence of the screening of the negative charge due to the interacting groups. The calculated frequency of the Oδ2-H stretching involved in the proton hopping is that which is characteristic of an LBHB (2470 cm^{-1}).[72]

During the dynamics, the dipole-charge interaction is completely maintained, as indicated by the Gly · · · Asp distance (d(NH · · · Oδ1) = 2.0(0.1), 2.3(0.3) Å) and by the large electrostatic interaction (approximately −11(3) kcal/mol), but the two peptides bonds experience significant rotation around the axis along the Cα atoms. Note that rearrangement could take place also in the real enzyme, because it is not sterically hindered by the protein frame. The dipoles interaction with the two carboxylates is very strong, and their rotation can, in turn, stabilize either the protonated or deprotonated form of the two groups, thus modulating the proton transfer process. This effect is expected to be important also during the catalytic process because it involves protonation and deprotonation of the aspartyl residues.

Hydration Effects

To investigate the role of the hydration on charge distribution and on proton dynamics, we performed simulations including a smaller number of water molecules. The timescale of proton hopping decreases to ~2 ps and to ~0.5 for the simulations with two and one water molecules, respectively. This indicates clearly that the solvent screens the charge of the active site rather effectively, thus further stabilizing the interactions between the negative groups.

A final remark is due on the influence of the water bridging the two Asp groups on the dynamics of the LBHB. In the three systems investigated, it is found that the proton is transferred only when this water forms two strong hydrogen bonds to the aspartyl residues; thus, the role of this water appears to achieve the correct geometry to render the carboxylate oxygens close enough for the transfer to occur.

Chemical Bonding

To characterize the nature of the chemical bonding during the proton transfer process we analyzed the electronic structure.

The analysis of the electronic structure is based on the centers of the maximally localized Wannier orbitals.[57,58] This type of analysis is revealing itself as a powerful tool to study the ionicity of chemical bonds, because the location of the centers can be related to the difference of Pauling electronegativity (Δ_χ) of the two atoms involved in the bond.[59] Here we apply this type of analysis to our largest model (**C**).

Figure 6 plots the Wannier centers of the H-Oδ1 bond in different chemical environments. In isolated, protonated Asp side chain the center is located roughly midway between the two atoms (Fig. 6b), indicating that the bond is significantly polarized toward the oxygen atom. The resulting difference of Pauling electronegativity (Δ_χ[OH] = 1.3), compares well with that found for water by Alber et al.[59] (Δ_χ[OH] = 1.2). In the active site of HIV-1 PR, the center is shifted toward the oxygen atom, indicating that the bond is very polar (Δ_χ[OH] = 2.0) (Fig. 6c). During the proton transfer (Fig. 6d), a further shift of the center toward the oxygen atoms reveals that the bond is essentially ionic. When the proton is bound to the second Asp residue (Fig. 6e), the character of the bond is similar to that of Fig. 6c, due to the symmetry of the system.

Therefore, we conclude that the aspartyl O-H bond is strongly polarized toward the oxygen and, during the proton transfer, the proton is almost completely unbound: the protomer can be described in terms of a $O^{\delta-} \cdots H^{+} \cdots O^{\delta-}$ complex. The strong ionic character of the O-H bonding may help explain the relative success in reproducing the structural properties of the active site with force field models in which the two Asp groups are considered deprotonated and a proton is located between the carboxylates.[28]

Environmental effects might induce significant polarization, because several charged residues relatively close to the active site of HIV-1 PR have been demonstrated to be crucial for the enzymatic function.[73]

To estimate qualitatively the polarization effects of the protein frame on the chemical bonding, we have calculated the shifts of the Wannier centers, including the protein electrostatic potential. As examples, we report the centers with and without the protein potential during the proton transfer (Fig. 7). The relative displacement of the Wannier centers toward the oxygen here is very small (0.006 Å), which corresponds to a very small change in bond ionicity ($\Delta_\chi[O_{\delta 1}H] \sim 0.06$ units). This applies also to all the other configurations investigated.

We conclude that, within our level of accuracy, the aspartyl O-H bond is strongly polarized toward the oxygen and, during the proton transfer, the proton is almost completely unbound. Thus, the protomer can be described in terms of a $O^{\delta-} \cdots H^{+} \cdots O^{\delta-}$ complex. The electric field of the protein frame does not play an important role in the proton transfer process because polarization effects are negligible (Fig. 7). The strong ionic character of the

O-H bonding may help explain the success in reproducing the structural properties of the active site with force field models in which the two Asp groups are considered deprotonated and a proton is located between the carboxylates.[28]

DISCUSSION AND CONCLUSIONS

Within the limitation of the short time scale explored and the size of the models used, our calculations provide information on the protonation state, on the proton location, and on the chemical physical origin of the stability of the Asp dyad in HIV-1 protease.

Our calculations show that the strong repulsion of the two negatively charged, closely opposed aspartyl residues in the deprotonated form is so large that unphysical rearrangements occur at the cleavage site.

Our findings that the Asp dyad conformation is not stable in the deprotonated form provides further support to the criticism of a recent NMR study,[30] which suggests the existence of the deprotonated form at pH 6. On the other hand, our calculations for the monoprotonated form, which suggest the presence of an almost ionic $-COO^{\delta-}H^{+}$ $-COO^{\delta-}$ complex, might explain the interpretation of the ^{13}C-NMR data in terms of two $-COO^{-}$ groups.

According to independent and consistent theoretical[46] and experimental[29] investigations, the Asp dyad shares one proton.

Our calculations predict that, in this protonation state, the conformation of a specific protonated form (**C** [Chart I]) is stable. Thus, within the limitation of our modeling, our results support the presence of the monoprotonated form in the protein and indicate the presence of an LBHB, as previously suggested by quantum dynamical calculations.[36]

Furthermore, we find that this LBHB and dipole-charge interactions help to fix the peculiar conformation of the Asp dyad.

Indeed, the close proximity of the two carboxylates is achieved by forming an LBHB, which overcomes the repulsion of the two negative residues.[70,71] The LBHB is characterized by rapid transfer of the shared proton, in agreement with previous suggestions based on quantum dynamical models.[36] The calculations presented here appear to provide a good description of the proton dynamics, because the calculated Oδ1(Asp25)-H vibrational frequency is in good agreement with those reported for a LBHB.[72] However, solvent effects and quantum fluctuations[74] might affect considerably the proton transfer properties of the LBHB.

Inclusion of the electric field of the entire protein does not significantly affect the electronic structure, suggesting that most important interactions necessary to describe adequately the conformation of the aspartyl pair and the proton transfer process are already included in the model. More sophisticated models of the electrostatic potential, which include, for instance, the polarizability, are expected to reduce the field and thus not to alter the picture.

The peculiar orientation of the two Asp residues is obtained through the interaction of the aspartyl negative charge with the rather rigid Thr 26(26′)-Gly 27(27′) peptide units' dipole. Recent site-directed mutagenesis experiments on the 27, 27′ position, which show the complete loss of catalytic power in the G27V, G27′V HIV-1 PR mutant,[1] appear to be consistent with the crucial role of this dipole. Indeed, replacing glycine with the bulk side chain of valine may cause a significant rearrangement of the backbone and thus of this dipole. This in turn may stabilize a conformation of the Asp dyad, which is not optimal for the catalytic action of the enzyme.

From the ab initio MD simulations, we have an indication that several ingredients, such as the polarization forces, the treatment of bond-forming/breaking processes, and temperature effects, play a crucial role in the HIV-1 PR active site. These ingredients are expected to play a critical role also in the adducts with substrate and inhibitors. On the basis of these findings, specific force fields could now be developed for this system, which in turn might allow for a more accurate modeling of HIV-1 PR-drug interactions.

ACKNOWLEDGMENTS

The authors thank Erio Tosatti and Michele Parrinello for their valuable comments on the manuscript.

REFERENCES

1. Bagossi P, Cheng YE, Oroszlan S, Tozser J. Activity of linked HIV-1 proteinase dimers containing mutations in the active site region. Protein Eng 1996;9:997–1003.
2. Debouck C, Gorniak JG, Strickler JE, Meek TD, Metcalf BW, Rosenberg M. Human immunodeficiency virus protease expressed in Escherichia coli exhibits autoprocessing and specific maturation of the gag precursor. Proc Natl Acad Sci USA 1987;84:8903–8906.
3. Kohl NE, Emini EA, Schleif WA, et al. Active human immunodeficiency virus protease is required for viral infectivity. Proc Natl Acad Sci USA 1988;85:4686–4690.
4. McQuade TJ, Tomasselli AG, Liu L, et al. A synthetic HIV-1 protease inhibitor with antiviral activity arrests HIV-like particle maturation. Science 1990;247:454–456.
5. Seelmeier S, Schmidt H, Turk V, von der Helm K. Human immunodeficiency virus has an aspartic-type protease that can be inhibited by pepstatin A. Proc Natl Acad Sci USA 1988;85:6612–6616.
6. Lapatto R, Blundell T, Hemmings A, et al. X-ray analysis of HIV-1 proteinase at 2.7 Å resolution confirms structural homology among retroviral enzymes. Nature 1989;342:299–302.
7. Wlodawer A, Miller M, Jaskolski M, et al. Conserved folding in retroviral proteases: crystal structure of a synthetic HIV-1 protease. Science 1989;245:616–621.
8. Navia MA, Fitzgerald PMD, McKeever BM, et al. Three-dimensional structure of aspartyl protease from human immunodeficiency virus HIV-1. Nature 1989;337:615–620.
9. McKeever BM, Navia MA, Fitzgerald PM, et al. Crystallization of aspartyl protease from the human immunodeficiency virus, HIV-1. J Biol Chem 1989;264:1919–1921.
10. Miller M, Schneider J, Sathyanarayana BK, et al. Structure of complex of synthetic HIV-1 protease with a substrate-based inhibitor at 2.3 A resolution. Science 1989;246:1149–1152.
11. Erickson J, Neidhart DJ, VanDrie J, et al. Design, activity, and 2.8 Å crystal structure of a C2 symmetric inhibitor complexed to HIV-1 protease. Science 1990;249:527–533.
12. Suguna K, Padlan EA, Smith CW, Carlson WD, Davies DR. Binding of a reduced peptide inhibitor to the aspartic proteinase from Rhizopus chinensis: implications for a mechanism of action. Proc Natl Acad Sci USA 1987;84:7009–7013.
13. Silva AM, Cachau RE, Sham HL, Erickson JW. Inhibition and catalytic mechanism of HIV-1 aspartic protease. J Mol Biol 1996;255:321–346.

14. Kempf DJ, Marsh KC, Denissen JF, et al. ABT-538 is a potent inhibitor of human immunodeficiency virus protease and has high oral bioavailability in humans. Proc Natl Acad Sci USA 1995;92: 2484–2488.
15. Sham HL, Zhao C, Stewart KD, et al. A novel, picomolar inhibitor of human immunodeficiency virus type 1 protease. J Med Chem 1996;39:392–397.
16. Jadhav PK, Ala P, Woerner FJ, et al. Cyclic urea amides: HIV-1 protease inhibitors with low nanomolar potency against both wild type and protease inhibitor resistant mutants of HIV. J Med Chem 1997;40:181–191.
17. Davies DR. The structure and function of the aspartic proteinases. Annu Rev Biophys Biophys Chem 1990;19:189–215.
18. Fitzgerald PMD, Springer JP. Structure and function of retroviral proteases. Annu Rev Biophys Biophys Chem 1991;20:299–320.
19. Todd MJ, Semo N, Freire E. The structural stability of the HIV-1 protease. J Mol Biol 1998;283:475–488.
20. Harte WE, Swaminathan S, Mansuri MM, Martin JC, Rosenberg IE, Beveridge DL. Domain communication in the dynamical structure of human immunodeficiency virus 1 protease. Proc Natl Acad Sci USA 1990;87:8864–8868.
21. Harte WE, Swaminathan S, Beveridge DL. Molecular dynamics of HIV-1 protease. Proteins Struct Funct Genet 1992;12:175–194.
22. York DM, Darden TA, Pedersen LG, Anderson MW. Molecular dynamics simulation of HIV-1 protease in a crystalline environment and in solution. Biochemistry 1993;32:1443–1453.
23. Wlodawer A, Vondrasek J. Inhibitors of HIV-1 protease: a major success of structure-assisted drug design. Annu Rev Biophys Biomol Struct 1998;27:249–284.
24. Chatfield DC, Brooks BR. HIV-1 protease cleavage mechanism elucidated with molecular dynamics simulation. J Am Chem Soc 1995;117:5561–5572.
25. Straatsma TP, Zacharias M, McCammon JA. Free energy difference calculations in biomolecular systems. In: van Gusteren WF, Weiner PK, Wilkinson AJ, editors. Computer simulations of biomolecular systems. Leiden: ESCOM; 1993. p 363.
26. Liu H, Muller-Plathe F, van Gusteren WF. A combined quantum/classical molecular dynamics study of the catalytic mechanism of HIV protease. J Mol Biol 1996;261:454–469.
27. Geller M, Miller M, Swansom SM, Maizel J. Analysis of the structure of HIV-1 protease complexed with a hexapeptide inhibitor. Part II. Molecular dynamic studies of the active site region. Proteins: Struct Funct Genet 1997;27:195–203.
28. Harrison RW, Weber IT. Molecular dynamics simulations of HIV-1 protease with peptide substrate. Protein Eng 1994;7:1353–1363.
29. Hyland LJ, Tomaszek TA Jr, Roberts GD, et al. Human immunodeficiency virus-1 protease. 1. Initial velocity studies and kinetic characterization of reaction intermediates by 18O isotope exchange. Biochemistry 1991;30:8454–8463.
30. Smith R, Brereton IM, Chai RY, Kent SBH. Ionization states of the catalytic residues in HIV-1 protease. Nature Struct Biol 1996;3:946–950.
31. Mavri J. Irreversible inhibition of the HIV-1 protease: a theoretical study. Int J Quant Chem 1998;69:753.
32. Hadzi D, Hodoscek M, Harb V, Turk D. Theoretical investigations of structure and enzymatic mechanism of aspartyl proteases. Part I. Ab initio calculations on an active site model: hydrogen diformate with H_2O and H_3O^+. J Mol Struct (Theochem) 1987;150:241–250.
33. Lee H, Darden TA, Pedersen LG. An ab initio quantum mechanical model for the catalytic mechanism of HIV-1 protease. J Am Chem Soc 1996;118:3946–3950.
34. Goldblum A, Glick M, Rayan A. Determining proton position in an enzyme-inhibitor complex is a first step for theoretical mechanistic studies of aspartic proteinases. Theor Chim Acta 1993;85:231–247.
35. Venturini A, Lopez-Ortiz F, Alvarez JM, Gonzalez J. Theoretical proposal of a catalytic mechanism for the HIV-1 protease involving an enzyme-bound tetrahedral intermediate. J Am Chem Soc 1998;120:1110–1111.
36. Berendsen HJC, Mavri J. Simulating proton transfer processes: quantum dynamics embedded in a classical environment. In: Hadzi D, editor. Theoretical treatments of hydrogen bonding. J Wiley & Sons: New York; 1997. p 119.
37. Beveridge AJ, Heywood GC. A quantum mechanical study of the active site of aspartic proteinases. Biochemistry 1993;32:3325–3333.
38. Car R, Parrinello M. Unified approach for molecular dynamics and density functional theory. Phys Rev Lett 1985;55:2471–2474.
39. Brooks CL, Karplus M, Pettit BM. Proteins: a perspective of dynamics, structure, thermodynamics. New York: John Wiley and Sons; 1988.
40. Becke AD. Density functional exchange-energy approximation with correct asimptotic behaviour. Phys Rev A 1988;38:3098–3100.
41. Lee C, Yang W, Parr RC. Development of the Colle-Salvetti correlation energy formula into a functional of the electron density. Phys Rev A 1988;37:785–789.
42. Parrinello M. From silicon to RNA: the coming age of ab initio molecular dynamics. Solid State Commun 1997;102:107–120.
43. Tuckerman ME, Laasonen K, Sprik M, Parrinello M. "Ab initio" molecular dynamics simulation of the solvation and transport of hydronium and hydroxyl ions in water. J Phys Chem 1995;99: 5749–5752.
44. Molteni C, Parrinello M. Glucose in aqueous solution by first principles molecular dynamics. J Am Chem Soc 1998;120:2168.
45. Alber F, Kuonen O, Scapozza L, Folkers G, Carloni P. Density functional studies on herpes simplex virus type 1 thymidine kinase-substrate interactions: the role of Tyr 172 and Met 128 in Thymine Fixation. Proteins Struct Funct Genet 1998;31:453–459.
46. Trylska J, Antosiewicz J, Geller M, et al. Thermodynamic linkage between the binding of protons and inhibitors to HIV-1 protease. Protein Sci 1999;8:180–195.
47. Case DA, Pearlman DA, Caldwell JW, et al. University of California, San Francisco: AMBER 5; 1997.
48. Berendsen HJC, Postma JPM, van Gunsteren WF, DiNola A, Haak JR. Molecular dynamics with coupling to an external bath. J Chem Phys 1984;81:3684–3690.
49. Troullier N, Martins JL. Efficient pseudopotentials for plane wave calculations. Phys Rev B 1991;43:1993–2006.
50. Barnett RN, Landman U. Born-Oppenheimer molecular dynamics simulations of finite systems: structure and dynamics of $(H_2O)_2$. Phys Rev B 1993;48:2081–2097.
51. Csaszar P, Pulay P. Geometry optimization by direct inversion in the iterative subspace. J Mol Struct 1984;114:31–34.
52. Hutter J, Ballone P, Bernasconi M, Focher P, Fois E, Godecker S, Parrinello M, Tuckerman M. CPMD version 3.0h. MPI für festkörperforschung and IBM Zurich research laboratory, 1995–1996.
53. Cox SR, Williams DE. Representation of the molecular electrostatic potential by a net atomic charge model. J Comput Chem 1981;2:304–323.
54. Bayly CI, Cieplack P, Cornell WD, Kollman PA. A well-behaved electrostatic potential based method using charge restraints for deriving atomic charges—the RESP model. J Phys Chem 1993;97: 10269–10280.
55. Cornell WD, Cieplack P, Bayly CI, Kollman PA. Application of RESP charges to calculate conformational energies, hydrogen bond energies, and free energies of solvation. J Am Chem Soc 1993;115:9620–9631.
56. Allen MP, Tildesley DJ. Computer simulations of liquids. Oxford, UK: Oxford Science Publications; 1986.
57. Marzari N, Vanderbilt D. Maximally localized generalized Wannier functions for composite energy bands. Phys Rev B 1997;56: 12847.
58. Silvestrelli PL, Marzari N, Vanderbilt D, Parrinello M. Maximally-localized Wannier functions for disordered systems: application to amorphous silicon. Sol State Comm 1998;107:7.
59. Alber F, Folkers G, Carloni P. "Dimethyl Phosphate: Stereoelectronic versus Environment Effect." J Phys Chem B 1999;103:6121–6126.
60. Rovira C, Carloni P, Parrinello M. The iron sulphur bond in cytochrome c. J Phys Chem B 1999;103:7031–7035.
61. Pauling L. General chemistry. New York: Dover Publications Inc.; 1988.
62. Polgar L, Szeltner Z, Boros I. Substrate-dependent mechanisms in the catalysis of human immunodeficiency virus protease. Biochemistry 1994;33:9351–9357.
63. Yamazaki T, Nicholson LK, Torchia DA, et al. NMR and X-ray evidence that the HIV protease catalytic aspartyl groups are protonated in the complex formed by the protease and a non-peptide cyclic urea-based inhibitor. J Am Chem Soc 1994;116: 10791–10792.

64. Tawa GJ, Topol IA, Burt SK, Erickson JW. Calculation of the relative binding free energies of peptidic inhibitors to HIV-1 protease and its I84V mutant. J Am Chem Soc 1998;120:8856–8863.
65. Harte WE, Beveridge DL. Prediction of the protonation state of the active site aspartyl residues in HIV-1 protease-inhibitor complexes via molecular dynamics simulation. J Am Chem Soc 1993;115:3883–3886.
66. Chen X, Tropsha A. Relative binding free energies of peptide inhibitors of HIV-1 protease: the influence of the active site protonation state. J Med Chem 1995;38:42–48.
67. Wang YX, Freedberg DI, Yamazaki T, et al. Solution NMR evidence that the HIV-1 protease catalytic aspartyl groups have different ionization states in the complex formed with the asymmetric drug KNI-272. Biochemistry 1996;35:9945–9950.
68. Hong L, Hartsuck JA, Foundling S, Ermoliff J, Tang J. Active-site mobility in human immunodeficiency virus, type 1, protease as demonstrated by crystal structure of A28S mutant. Protein Sci 1998;7:300–305.
69. Murty KHM, Winborne EL, Minnich MD, Culp JS, Debouck C. The crystal structures at 2.2-A resolution of hydroxyethylene-based inhibitors bound to human immunodeficiency virus type 1 protease show that the inhibitors are present in two distinct orientations. J Biol Chem 1992;267:22770–22778.
70. Cleland WW, Kreevoy MM. Low-barrier hydrogen bonds and enzymic catalysis. Science 1994;264:1887–1890.
71. Frey PA, Whitt SA, Tobin JB. A low-barrier hydrogen bond in the catalytic triad of serine proteases. Science 1994;264:1927–1930.
72. Bertolasi V, Gilli P, Ferretti V, Gilli G. Evidence for resonance-assisted hydrogen bonding: intercorrelation between crystal structure and spectroscopic parameters in eight intramolecularly hydrogen bonded 1,3-diaryl-1,3-propanedione enols. J Am Chem Soc 1991;113:4917–4925.
73. Loeb DD, Swanstrom R, Everitt L, Manchester M, Stamper SE, Hutchinson CA. Complete mutagenesis of the HIV-1 protease. Nature 1989;340:397–400.
74. Tuckerman ME, Marx D, Klein ML, Parrinello M. On the quantum nature of the shared proton in hydrogen bonds. Science 1997;275:817–820.
75. Nelson RD, Lide DR, Maryott AA. Selected values of electric dipole moments for molecules in the gas phase. In: Weast RC, editor. Handbook of Chemistry and Physics. CRC Press Inc.: Boca Raton, FL; 1982.